Effect of intermittent operation on the thermal efficiency of energy tunnels under varying tunnel air temperature.

Oluwaseun Ogunleye[1]; Rao Martand Singh[1]; Francesco Cecinato[2]; Jung Chan Choi[3]

[1]*Department of Civil and Environmental Engineering, Faculty of Engineering and Physical Sciences, University of Surrey, Guildford, GU2 7XH, UK.*

[2] *Dipartimento di Scienze della Terra "Ardito Desio", Università degli Studi di Milano, via Mangiagalli 34, 20133 Milan,* Italy.

[3] *Norwegian Geotechnical Institute (NGI), Oslo, Norway P.O. Box. 3930 Ullevål Stadion, N-0806 Oslo, Norway.*

Corresponding author's email: r.singh@surrey.ac.uk

Abstract

This paper focusses on hot underground tunnels and studies the effect of ground source heat pump (GSHP) intermittent operation and changing tunnel air temperature profile on energy tunnel thermal efficiency. The effects of heat pump operation on the tunnel surrounding soil and the soil recovery rate when the heat pump is not in operation were also studied. A 3D numerical model was developed to simulate the transient heat transfer intermittent operation of an energy tunnel. The intermittent operation was reproduced by controlling the convective heat flux at the boundary between the absorber pipe and the tunnel lining. Variation in the tunnel air temperature was defined in the model as a periodic sink amplitude. Results show that in energy tunnels strategic intermittent operation increases thermal efficiency and allows the surrounding soil to thermally recover and prevent any adverse effect on the system. A high daily intermittent operation ratio increases the average thermal output but might lead to higher operating costs. Therefore, for a given site, it is important to determine the optimum intermittent ratio. The paper also shows how the variation in tunnel air temperature affects the thermal performance of the energy tunnel. The importance of including this variation (rather than assuming a constant average value) when estimating the geothermal potential of underground tunnels was also highlighted. Insights are also provided on the soil temperature recovery rates after prolonged operation. These would serve as a basis for working out a seasonal intermittent operation strategy to optimise the use of ground source heat pumps in underground tunnels.

Keywords

Geothermal energy; Energy tunnel; GSHPs; Energy efficiency.

1. Introduction

Ground heat exchanger (GHE) systems designed for space heating/cooling are emerging as a more thermally efficient, cost effective and cleaner alternative to fossil fuel-based heating systems. Pile heat exchangers (PHEs) and (to a smaller extent) retaining/diaphragm wall heat exchangers (WHEs) are the most common underground structural heat exchangers; however, there is a growing interest in the thermal activation of tunnels due to a larger area that could be thermally activated compared to PHEs and WHEs. GSHP used in tunnels system takes advantage of the relatively constant year-round underground temperature. In energy tunnels **(Fig. 1)**, the tunnel lining is equipped with heat

absorbing pipes where water with/without anti-freeze is circulated, exchanging heat with the surrounding materials. The heat absorbed is then transferred into the building via a heat pump for space heating/cooling and/or hot water. In hot tunnels, where the yearly average temperature inside the tunnel is significantly higher than the outside air temperature (due to the heat generated in the tunnel for various reasons), the heat flux from the tunnel represents an additional source of thermal energy [1]. However, there is little knowledge about the effect of tunnel air temperature and intermittent operation on the thermal performance of energy tunnels, which motivates the present study.

The first thermo-active tunnel was built in Austria, as absorber tubes were installed whilst upgrading the Lainzer tunnel through Vienna in 2004. This was done as a demonstration for a larger research project. It was projected that 214 MWh of energy could be achieved during one heating period [2]. Austria also has plans to use geothermal energy from tunnels along new railway lines [3]. Other countries have followed suit, most recently in Italy where an energy tunnel prototype was realised in the Turin Metro Line 1 South extension [4]. However due to the high energy costs of providing ventilation inside hot underground tunnels, new tunnel ventilation designs are being proposed [5]. Operation of energy tunnels can serve as a cheaper supplementary cooling option for underground tunnels requiring ventilation, as this can be achieved during the heat extraction cycle of the system [6]. However, some tunnel ventilation may still be required for fire-safety reasons.

The majority of existing research has focused on BHE and PHE, however the results and assumptions from these studies are not adequate to describe the operation of an energy tunnel due to the difference in geometry and boundary conditions. Hot tunnels are more efficient when used for heat extraction [1], while injecting heat during the hot season is potentially less suitable [7], since some of these tunnels (rail and metro tunnels) already require ventilation for comfort reasons. This paper focusses on heat extraction during the cold season and studies the effect of varying air temperature on energy tunnel efficiency (previous studies assume constant seasonal average temperature). The paper also investigates whether the heat flux from the tunnel is enough to thermally recharge the soil or an intermittent operation should be considered. The effect of different daily intermittent ratios (IR, i.e. the ratio between the heat pump off period and the on period) and seasonal heating on the surrounding soil and thermal performance of the energy tunnel is also investigated. Simulations were carried out for a 90 day period immediately after heat extraction. This was done to gather information about the soil recovery rate. These results would serve as a basis for working out seasonal optimum intermittent operation in energy tunnel to improve efficiency, which has not been considered yet.

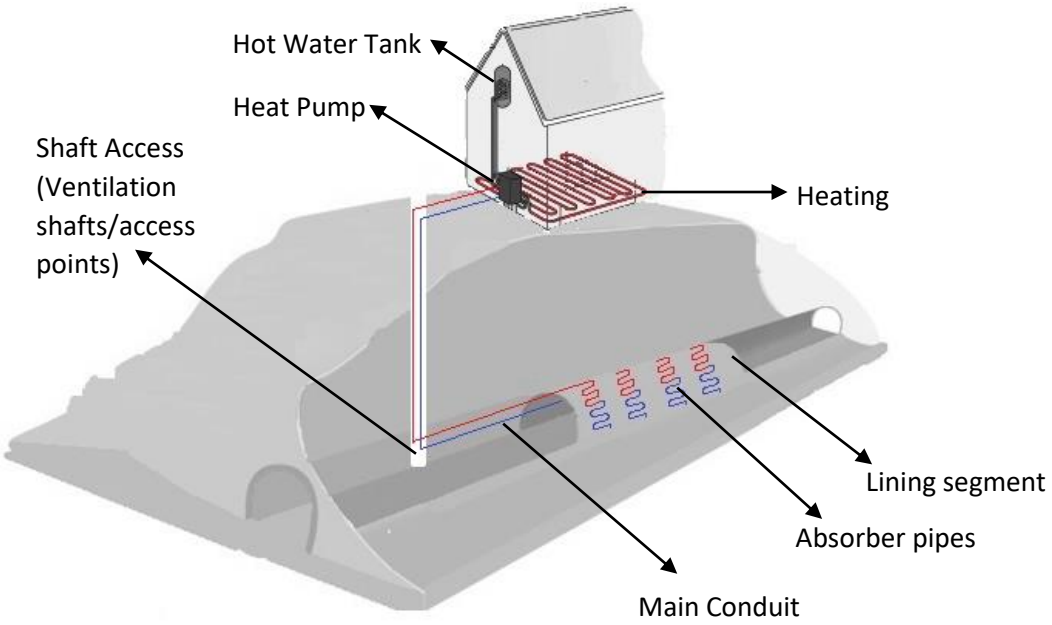

Fig. 1. Schematic of an energy tunnel.

2. Background

Recent studies on energy tunnels have shown interesting observations on the thermal performance of these energy geostructures. The field scale energy tunnel prototype realised in Turin Metro in Italy ("Enertun") is a good example, capable of extracting 51.30 W/m^2 of thermal power [4]. A novelty in this project was the placement of absorber pipes perpendicular to the tunnel axis, which yielded a reduction in hydraulic head loss and increased efficiency (due to the presence of flowing groundwater). Heat waste recovery from London underground (LU) using heat pumps was the focus of Davies et al. [8]. They proposed a combined cooling and heat recovery system to reverse the rising temperature in LU and also for use in district heating. It was estimated that the system could provide 900 kW of cooling to the tunnel and after upgrading the extracted heat, the system could potentially provide 1.1 MW of heat for district heating.

Most underground tunnels can be used as energy tunnels; however in traffic tunnels the air temperature changes due to the heat generated by electrical and mechanical equipment and also due to the movement of trains or vehicles (which accounts for the majority of the heat load inside underground rail tunnels). Some of the heat generated is transferred to the tunnel wall [9-11]. To study the effect of tunnel air on the thermal output of GHEs, knowledge of the boundary condition at the tunnel lining air interface is important. A good understanding of the flow profile and the convective heat transfer coefficient is also essential, as the convective heat transfer coefficient might vary due to activities inside the tunnel, e.g. frequency of train movements. However, few publications focus on the airflow and temperature profile inside underground tunnels. Sadokierski and Thiffeault [12] developed an analytical solution for the turbulent air flow in an open tunnel and annulus between the wall and a moving train to study soil thermal response to impulse and periodic variation in heat transfer coefficient and air temperature. The analytical solutions developed were applied to data obtained from Piccadilly line station in London, the results showed that for a periodic variation in air temperature, the thermal gradient along the tunnel changes with the air

temperature. Wall temperature and air temperature exhibits the same period, but with different amplitudes and a slight lag. However, a phase shift and reduction in the magnitude of the temperature oscillations is noticeable away from the tunnel surface**.** The polynomial regression of the tunnel air temperature measurements taken from underground tunnels reveal a periodic oscillation, as illustrated in **Fig. 2** and Season

Fig. 3. The plots show the tunnel air temperature measured from Stuttgart–Fasanenhof in Germany, Jenbach tunnel in Austria [1] and metro Torino in Italy [13]. The effect of fluctuating tunnel air temperature on the performance of GHEs installed in Stuttgart–Fasanenhof in Germany was studied by Buhmann et al. [1]; measuring instruments were installed in the tunnel, showing that varying tunnel air temperature affects the heat flux density in the tunnel and hence the extraction rate. Despite these observations the effect of tunnel air fluctuation and intermittent operation on the energy tunnels efficiency has not been extensively explored.

One major problem with the continuous operation of ground source heat pump systems (GSHPs) is the potential for ground temperature alterations compared to the undisturbed value, which could have an impact on the system's thermal efficiency. In addition, geothermal projects must comply with local environmental regulations due to potential risk of altering ground properties around nearby buildings [3]; in fact, the continuous operation of energy tunnels could result in undesirable thermal effects in the surrounding soil. Intermittent operation of the GSHPs could alleviate this problem with studies showing that GSHP systems benefit from intermittent operation [14]. The majority of literature work has focussed on PHEs and borehole heat exchangers (BHEs) and some of the findings are highlighted in this section. Considering studies carried out using experimental methods, Faizal et al. [14] investigated the effect of intermittent and continuous cooling operation in a geothermal pile. Their results show that the average soil temperature around the pile increases at shorter operating hours leading to an increase in energy extracted. An experiment was also carried out by Lu et al. [15] to compare the effect of operating under different IRs on the efficiency of a ground source heat pump. The thermal performance of the system improved for higher IR, while it worsened at lower IR.

Considering analytical solutions, Zhang et al. [16] developed an analytical model for a composite medium to simulate the intermittent operation of a GSHP. The model assumes that heat flux was constant during operation and zero during the off periods. Their results showed that an IR less than 0.5 restores the ground temperature to within 95% of the original value and smaller modulation of the intermittent time period is less efficient compared to higher modulation. This observation is contrary to other studies (e.g. [17]), where the short time interval intermittent operation mode was shown to improve the GHE's performance compared to long time operation. This observation was also supported by Liu et al. [18], who showed that a short modulation of the intermittent operation time in a cycle stabilises the outlet water temperature thus increasing efficiency. The temperature response of a soil with groundwater flow surrounding a BHE in intermittent operation was also studied analytically by Zhang et al. [19]. It was observed that after 5 days of continuous operation the surrounding soil temperature had increased significantly relative to the intermittent operation and also that higher ground water flow velocity helped the soil to recover more quickly during off periods. Li et al. [20] analytically investigated the effect of 5 years of intermittent operation (4 months on, 8 months off) of a BHE on its coefficient of performance (COP), the conclusion from their studies shows that the BHE performs better under intermittent operation.

Numerical models have also been developed to investigate the benefits of intermittent operation. Yang et al. [21] developed a 3D numerical model to simulate a GSHP system with groundwater advection. The result of the simulation shows an improvement in thermal efficiency due to the

intermittent operation. In addition, using numerical modelling, Zarrella et al. [22] studied the seasonal efficiency of a GSHP with helical heat exchangers operating at three different modes: intermittent (1 hour on and 1 hour off), continuous day (pump works between 7 am and 7 pm) continuous night (pump works between 7 am and 7 pm). The average seasonal efficiency was approximately the same for all the operating modes. Chen et al. [23] developed a numerical model to compare the efficiency and payback periods of a GSHP system running under continuous condition and two different intermittent conditions in a three years period. Intermittent operation decreases the rate of heat accumulation. The operating cost was also found to be lower when the system was operated intermittently and also there was an increase in energy efficiency ratio (EER). A similar study was reported by He and Sun [24]. The energy consumption during intermittent heating was calculated and found to be lower than the continuous mode, reportedly saving about 1120 tonnes of fuel per year and reduced water pump consumption by 240000 kWh/ year. In some cases, phase change materials (PCMs) are combined with grout to improve the efficiency of the ground source heat pump. Chen et al. [25] carried out a research on the effect of intermittent operation on PCM. The objective was to determine whether PCM can return to its initial state during the off period. A high IR of 2 was recommended to avoid excessive thermal stress and also to ensure that the PCM returns to its original state.

Heat pump working conditions (i.e. condensing temperature and evaporating temperature) can be optimised from the knowledge of the ideal IR which in turn increases the efficiency of the GSHP system [26]. The mean heat exchange rate of a GHE is higher in intermittent operation compared to continuous operation which makes it more efficient with regards to energy performance and soil temperature variation [27-33]. For soil with high thermal conductivity the rate of soil thermal recovery increases during intermittent operation, which improves the performance of the GHE [34]. However for a spiral-coil GSHP, Li et al. [35] showed that for an intermittent operation where there is a day-high/night-low operation load the system would perform better under continuous operation. The area affected by the heating and cooling of the soil due to action of the GSHPs decreases as the IR increases as reported by Cao et al. [36], and intermittent operation allows soil surrounding the GHEs to undergo thermal recovery hence an increase in COP as found by Liu et al. [18].

Continuous cyclic heating and cooling operation of the GSHP can lead to heat or cold accumulation in the surrounding soil and also induce potentially detrimental thermo-mechanical effects on the geo-structures and surrounding soil [14]. Running the heat pump in intermittent mode could be one of the solutions to mitigate this effect. However, since most research carried out so far has focused on BHE and PHE, the results and assumptions from these studies are not adequate to describe the operation of an energy tunnel, due to the difference in geometry and boundary conditions.

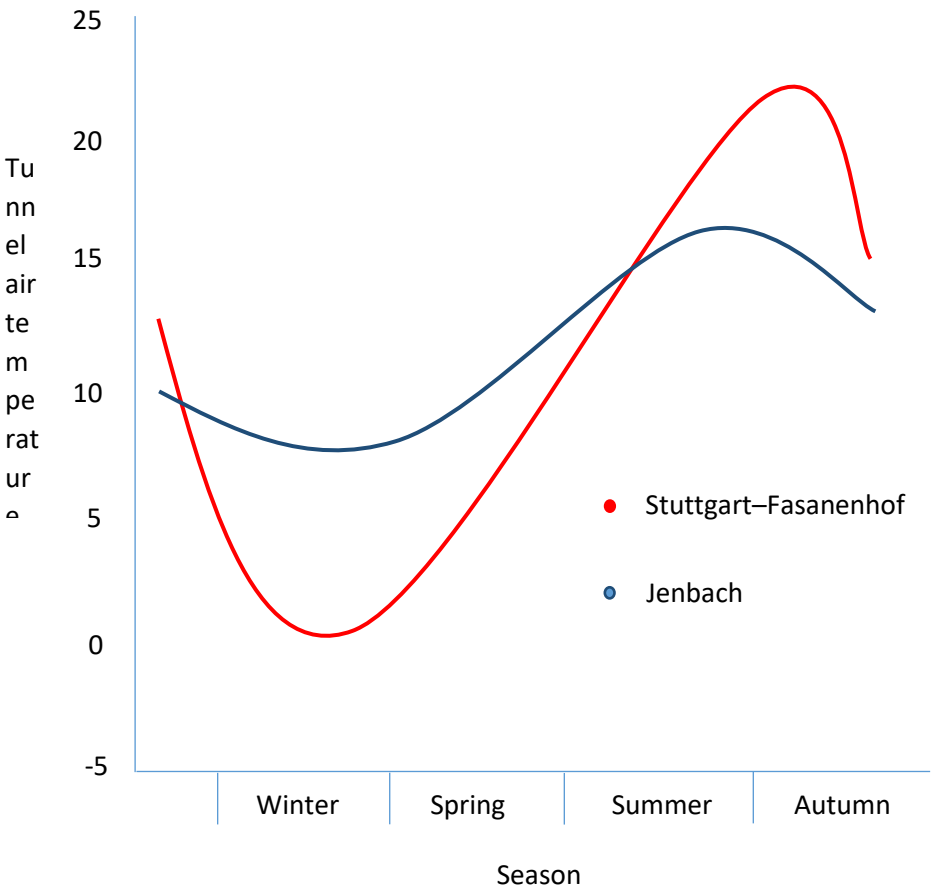

Fig. 2. Polynomial regression of the tunnel temperature at Jenbach and Stuttgart–Fasanenhof [1].

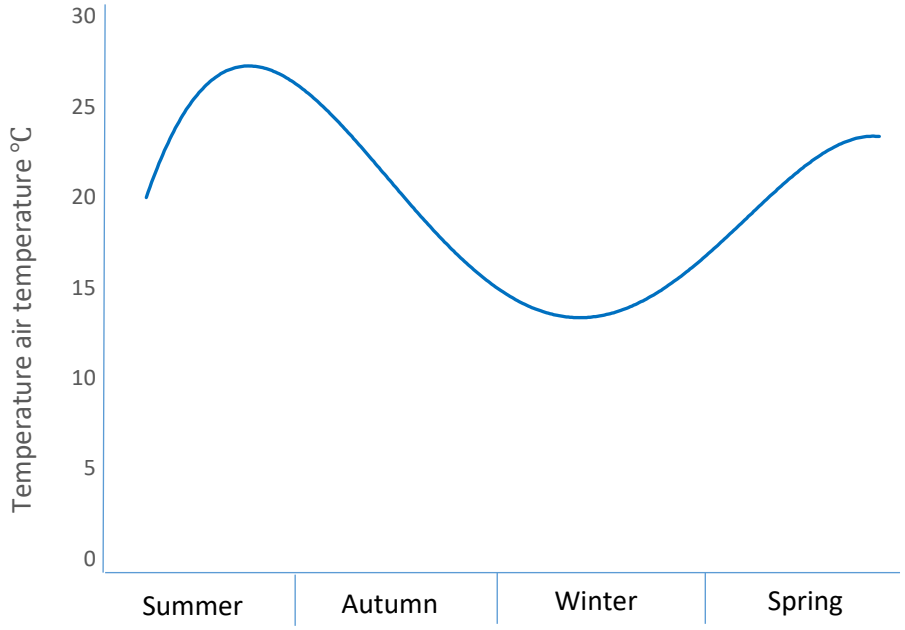

Season

Fig. 3. Polynomial regression of the tunnel temperature measured at metro Torino Italy [13].

3. Methodology

In this study, a transient 3D numerical model capable of simulating both cooling and heating operation of an energy tunnel was developed and validated using experimental results (Section 5). In the subsequent numerical study (Section 6), the system is considered as operating under daily intermittent conditions when it is in operation for less than 16 hrs per day, while it is considered as operating under continuous conditions when it is in operation for more than 16 hrs. The IR is defined as the ratio between the off period and the on period. For example, if the heat pump is in operation for 8 hrs and off for 16 hrs within a 24 hr period, the IR is 16/8 = 2.

The 3-D finite element numerical model was developed using the finite element software ABAQUS, with bespoke user subroutines (FILM and URDFIL). Subroutine "FILM" allows users to define non-uniform heat transfer coefficient and associated sink temperature, while "URDFIL" is used to read the ABAQUS result files during an analysis. The model was developed to simulate diffusive and convective heat transfer in heat absorber pipes, heat diffusion in the energy tunnel lining and surrounding soil with no groundwater flow, for either cooling or heating operation of the GHEs. In fact, this study is focused on energy tunnels excavated in clayey soil (as is often the case, for example, in the London area) and in dry granular soils. However, the model could be easily extended to also account for groundwater convection.

In this study, all parts in the model are assumed to have constant properties (density, specific heat capacity and thermal conductivity) with negligible thermal contact resistance at the interface between tunnel lining and the surrounding soil and between the tunnel lining and the absorber pipe. The soil was modelled as homogeneous, fully saturated with no groundwater flow. The conductive heat transfer of the fluid along the pipe axis was considered negligible and also the radiation heat transfer in soil was neglected, see [37]. Therefore, the main heat transfer phenomena considered in the model are listed as follows: conduction heat transfer in concrete lining; conduction heat transfer in ground; convective heat transfer between the circulating fluid and the pipe wall; convective heat transfer between the tunnel air and the tunnel lining.

The transient conduction heat transfer in concrete lining and conduction heat transfer in ground is governed by Fourier's law [38], as shown in **Eq. (1):**

$$q'' = -k\frac{\partial T}{\partial n}n \tag{1}$$

where q'' is the heat flux in in the direction of a unit vector n , T is the temperature, k is the thermal conductivity. In Cartesian coordinates [38], the transient heat equation may be written as:

$$\frac{\partial^2 T}{\partial x^2}+\frac{\partial^2 T}{\partial y^2}+\frac{\partial^2 T}{\partial z^2}+\frac{q}{k}=\frac{1}{\alpha}\frac{\partial T}{\partial t} \tag{2}$$

where t is the time and α is the thermal diffusivity.

The heat transfer between the tunnel air and the tunnel lining is described by a convection surface condition [31] and thus may be written as:

$$-k_L \frac{\partial T}{\partial n} = h[T_L - T_\infty] \tag{3}$$

where h is the convective heat transfer coefficient between the tunnel air and the tunnel lining, T_L is the temperature of the tunnel lining around the pipe, T_∞ is the air temperature, k_L is the thermal conductivity of the tunnel lining.

Similarly for the convective heat transfer between the circulating fluid and the pipe wall, assuming that the conductive heat transfer of the fluid along the pipe axis is negligible, we can assume a radial heat transfer at the boundary between the absorber pipe and the tunnel lining. The convective boundary condition at this surface can be expressed as follows [31]:

$$-k_L \frac{\partial T}{\partial n} = h_{eq}[T_L - T_f] \tag{4}$$

where T_f is the working fluid temperature, and h_{eq} is the equivalent convective heat transfer coefficient, as proposed by [31] to simplify the model by combining the thermal resistance of the pipe wall and working fluid's convective heat transfer coefficient:

$$h_{eq} = \left[\frac{D_{out}}{2k_{pipe}} \ln\left(\frac{D_{out}}{D_{in}}\right) + \frac{D_{out}}{D_{in}h}\right]^{-1} \tag{5}$$

In the above, k_{pipe} is the thermal conductivity of the pipe, h is the convective heat transfer coefficient of the working fluid, D_{out} and D_{in} are the outer and inner pipe diameters respectively.

To determine the temperature variation along the pipe, assuming the working fluid is incompressible and also moving at constant flow rate in a pipe of finite length, the thermal energy equation can be expressed as [38]:

$$q''\pi DL = \dot{m}C_p(T_{out} - T_{in}) \tag{6}$$

If **Eq. (6)** is applied to the control volume shown in **Fig. 4** and we integrate over the cross section this gives:

$$dq = q''\pi Ddl = \dot{m}C_p(T_m + dT_m) - T_m = \dot{m}C_p(dT_m) \tag{7}$$

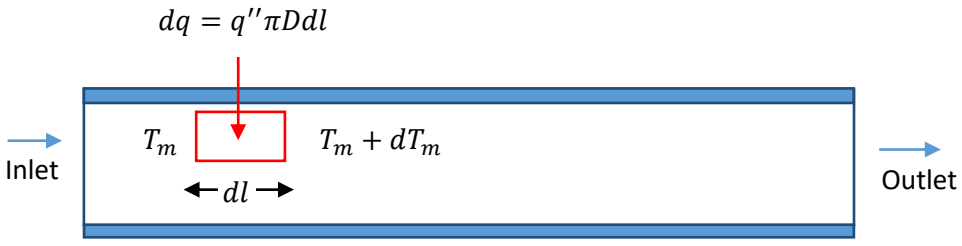

Fig. 4. Control volume for the flow in the absorber pipe.

3.1. Numerical modelling

A 3-D model of a single tunnel ring was considered in the simulation to reduce complexity and computational time. This assumption is valid in the absence of ground water flow or with groundwater flow perpendicular to the tunnel axis, since adjacent rings would not affect each other from a thermal point of view. To solve the 3-D transient heat transfer problem, linear hexahedral elements were used, while a finer mesh was used around the absorber pipe to improve accuracy**.**

It should be noted that pipes are represented within the 3D mesh as lines of nodes, however, the 3D nature of pipes is properly accounted for by means of the user subroutines, accounting for the surface area of each pipe segment, see [37, 39], the steps followed are summarised using the flowchart presented in **Fig. 5**. In order to calculate the temperature variation along the pipe, **Eq. (7)** can be written in terms of element node *i* as:

$$q''\pi Ddl = \dot{m}C_p(T_{i-1}) - T_i \tag{8}$$

Rearranging **Eq. (8)** to find the fluid temperature at node *i* gives:

$$T_i = T_{i-1} - \frac{q''\pi Ddl}{\dot{m}C_p} \tag{9}$$

The fluid flow simulation uses **Eq. (9)** to calculate the fluid temperature at any time step and at each node along the heat exchanger pipe.

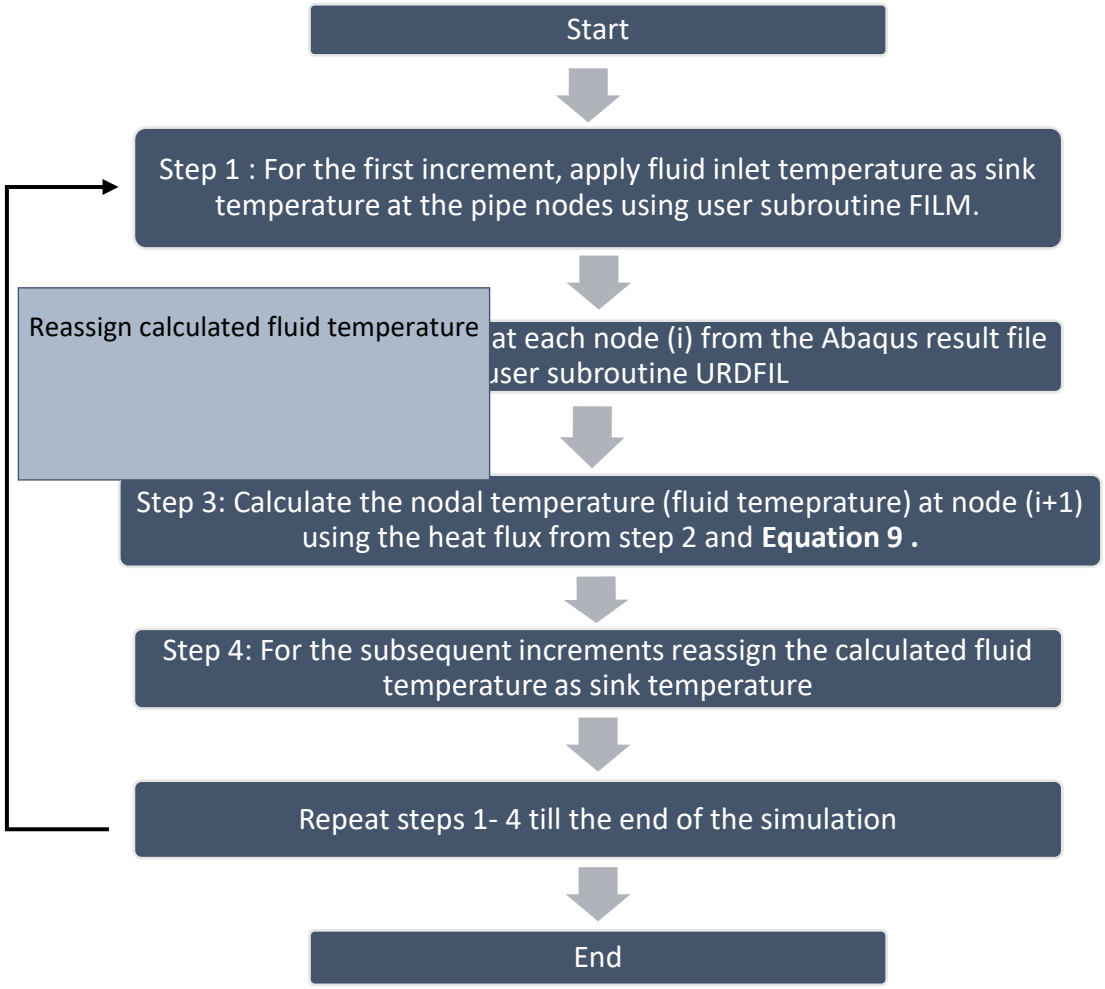

Fig. 5. Flow chart showing the program flow.

3.2. Model validation

The domain geometry created for model validation is presented in **Fig. 6,** the size of the domain was adequate for the duration considered (no temperature change at the boundary)**.** The initial temperature for the whole domain was set to 5.6°C, this corresponds to the undisturbed ground temperature around the tunnel.

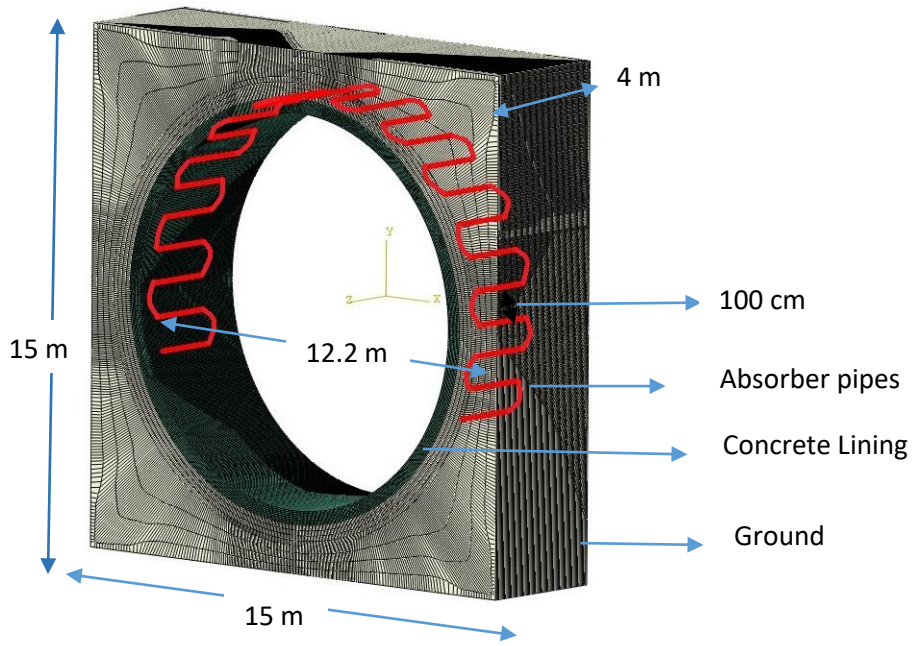

Fig. 6. Geometry and dimensions for model validation

The material parameters used in the numerical analysis are presented in Errore. L'origine riferimento non è stata trovata..

Table 1. Test data for Linchang Tunnel

Parameter	Value
Inner diameter of the tunnel	11.40 m
Thickness of the secondary Lining	400 mm
Pipe spacing	1 m
Pipe Length	50 m
Absorber pipe outer diameter and wall thickness	25 mm, 2.3 mm
Heat transfer coefficient inside the tunnel	15 W/m^{2}K
Inlet fluid temperature	20°C
Tunnel air temperature	10°C
Surrounding rock temperature	5.6°C

Material Properties:

	Thermal conductivity (W/m K)	Density (kg/m^3)	Specific heat (J/kg K)	Kinematic viscosity
Circulating fluid	0.56	1000	4200	1.3×10^{-6} m^2/s
Concrete lining	1.85	2400	970	
Surrounding rock	3.22	2544	1293	

The numerical results waere compared to the experimental results in terms of measured outlet fluid temperature, as shown in **Fig. 7.** The simulation showed good agreement with the experimental measurements by Zhang et al. [40], thus it can be deduced that the numerical model can correctly

reproduce both transient and quasi-steady state phases of heat transfer over a period of 50 hours of continuous cooling**.**

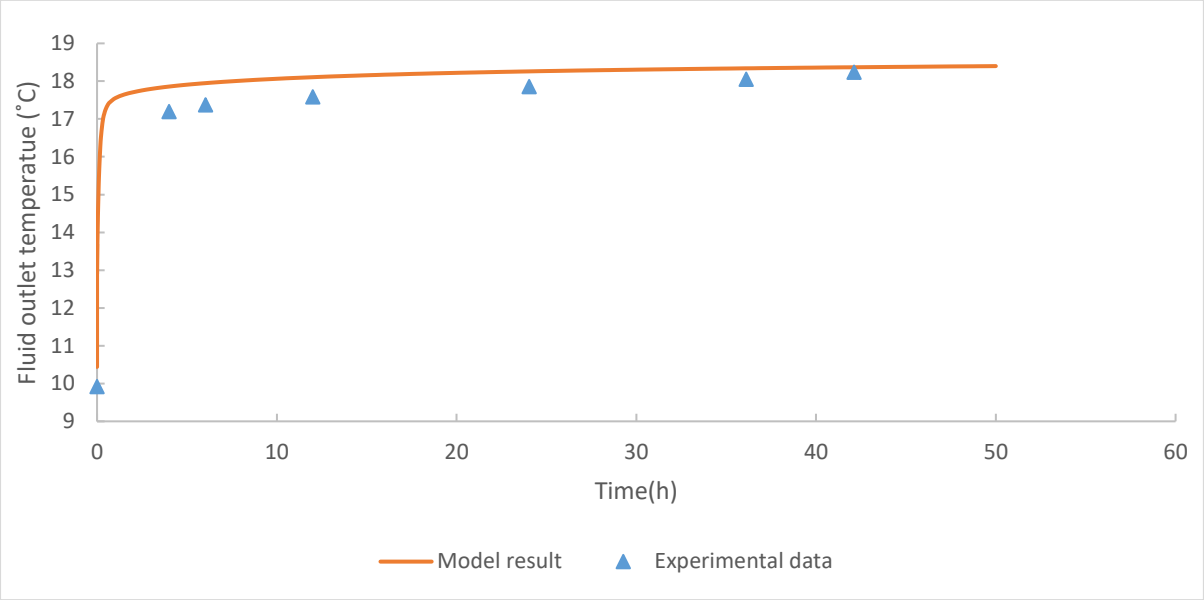

Fig. 7. Model validation with experimental result from Linchang tunnel.

3.3. Parametric numerical study

This section describes the use of the model for a parametric analysis to investigate the effect of air temperature and intermittent operation on an energy tunnel's cooling operation. Several simulations were carried out, using the physical and thermal properties listed in **Table 2.** These were chosen among typical values representing energy tunnel projects, as emerging from the literature discussed in Section 2.

The heat capacity and thermal conductivity of the concrete lining were taken from the values published by Barla et al. [13]. However, it should be remarked that the soil's thermal properties are site specific. For example, the soil thermal conductivity can vary between 0.1 – 5 W/m K depending on the water content and mineralogy [41]. In our simulations the soil heat capacity and thermal conductivity were given values of 2.8 W/m K and 2.0 MJ/kg K respectively, as these values lie within the ranges published by Clarke et al. [41], as well as being comparable to the values reported by Buhmann et al. [1]. High density polyethylene is commonly used for the absorber pipe with an external diameter of 20 – 25 mm and thickness of 2 – 2.3 mm [2]. In order to achieve turbulent flow within the pipe using the diameter range specified above, fluid velocities between 0.4 – 1.2 m/s are typically chosen [37]. A pipe diameter of 20.4mm and fluid velocity of 0.4 m/s were chosen in our analysis, yielding a Reynolds number of 8160, hence corroborating turbulent flow.

The geometry of the tunnel was taken from Barla et al. [13] as an example. The intermittent operation cycles considered are based on typical intermittent cycle of GSHPs as discussed in Section 2. Concerning the convective heat transfer coefficient between tunnel lining and the tunnel air, values between 6 W/m^{2}K and 20 W/m^{2}K have been suggested depending on the air velocity inside the tunnel [7].

3.3.1. Initial conditions

Measurements from underground tunnels have revealed the presence of an initial temperature gradient around the soil closer to the tunnel lining, due to heat exchange between the tunnel air and tunnel wall. At Stuttgart–Fasanenhof tunnel in Germany, a maximum difference of 5.5°C near the tunnel lining was measured relative to the undisturbed ground temperature, the area affected by the initial temperature disturbance was measured to extend to 7 m from the external lining [1]. The maximum temperature difference between tunnel lining and undisturbed ground may also increase over years after tunnel construction, as reported by Wang et al. [42]. However, the effect of the initial temperature field is negligible for long term applications, once the operation reaches steady state [43]. For the purpose of this study, the initial temperature of the ground was considered to be 14°C, corresponding to the undisturbed ground temperature.

3.3.2. Boundary conditions

In order to study the effect of the tunnel air flow and temperature on the thermal output of the energy tunnel, the tunnel air temperature data shown in Fig. 3 were applied in the model as boundary conditions **(Fig. 8)**. Tunnel heating operation was simulated for a total of 180 days (December to May) using an analogous procedure as that presented above for cooling operation. The simulation steps can be subdivided into two phases: 90 days of heat extraction (December to February); 90 days without heat extraction (March to May).

A 90 days heating period, from December to February, was selected for simulation as this is the highest heating demand period. The corresponding temperature variation was defined in the model as a periodic sink amplitude. A constant convective heat transfer coefficient was considered for simplicity, selecting a realistic average value of 15 W/m^{2}K, based on published values [7, 40].

With the aim of studying the effect of intermittent operation on the energy tunnels output the following daily intermittent cycles were simulated: 16 hours on 8 hours off (IR = 0.5); 12 hours on 12 hours off (IR = 1); 8 hours on 16 hours off (IR = 2)

The water inlet temperature was given a value of 4°C along the lines of [13].

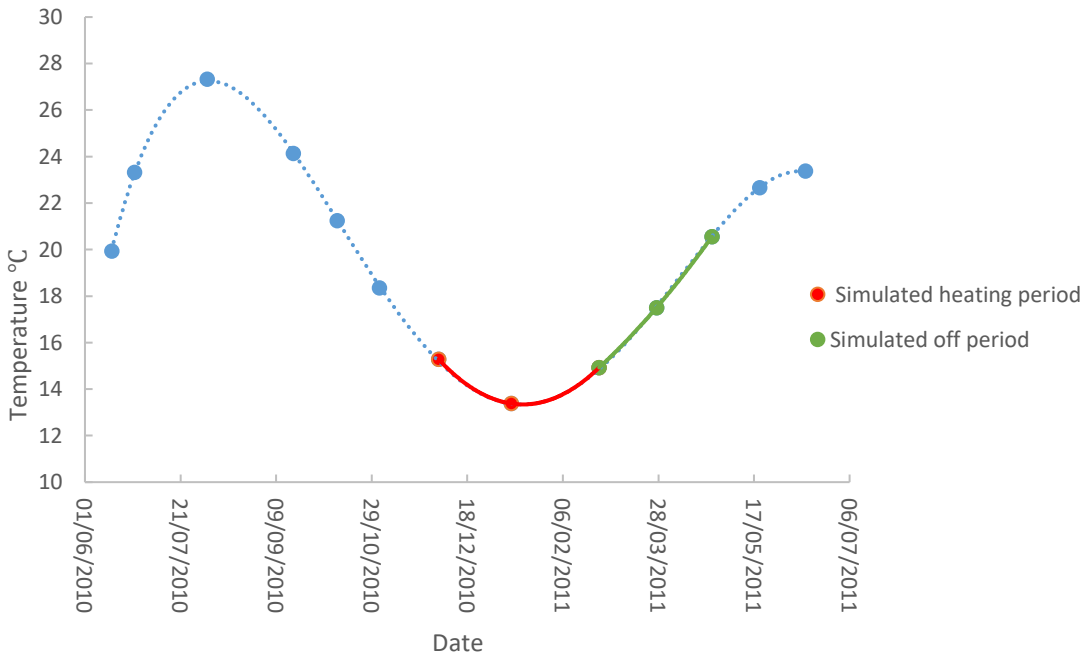

Fig. 8. Tunnel temperature data, showing the simulated heating and cooling period.

Some of the important material parameters used for the numerical analysis are presented in **Table 2**:

Table 2. Numerical simulation parameters.

Parameter	Value
Tunnel diameter	6.8 m
Tunnel lining thickness	300 mm
Maximum tunnel overburden measured from the tunnel centre	21.5 m
Absorber pipe outside Diameter, pipe thickness, spacing	25 mm, 2.3 mm, 300 mm
Total number of ring considered	1
Inlet temperature:	4˚C
Initial soil temperature	14˚C
Heat transfer coefficient between tunnel air and lining	15 W/m^{2}K
Working fluid flow velocity	0.4 m/s
Absorber pipe Thermal conductivity	0.385 W/m K

Material Properties:

	Thermal conductivity (W/m K)	Heat Capacity (MJ/kg K)
Circulating fluid	0.53	4.2
Concrete lining	2.3	2.19
Surrounding soil	2.8	2.0

3.3.3. Geometry and discretisation

The domain size is 43 m x 43 m x 2 m **(Fig. 9)**. The size of the geometry was adequate for the intermittent operations considered (no significant temperature change at the external boundary). A mesh dependency numerical study was carried out to determine the sufficient number of elements to obtain convergence, and a finer mesh was used around the absorber pipe. The study was carried out with the parameters in **Table 2** in continuous operation mode. The steady state outlet temperature in continuous mode converged at 184400 elements as shown in **Table 3**, hence a solution independent of the mesh size was achieved.

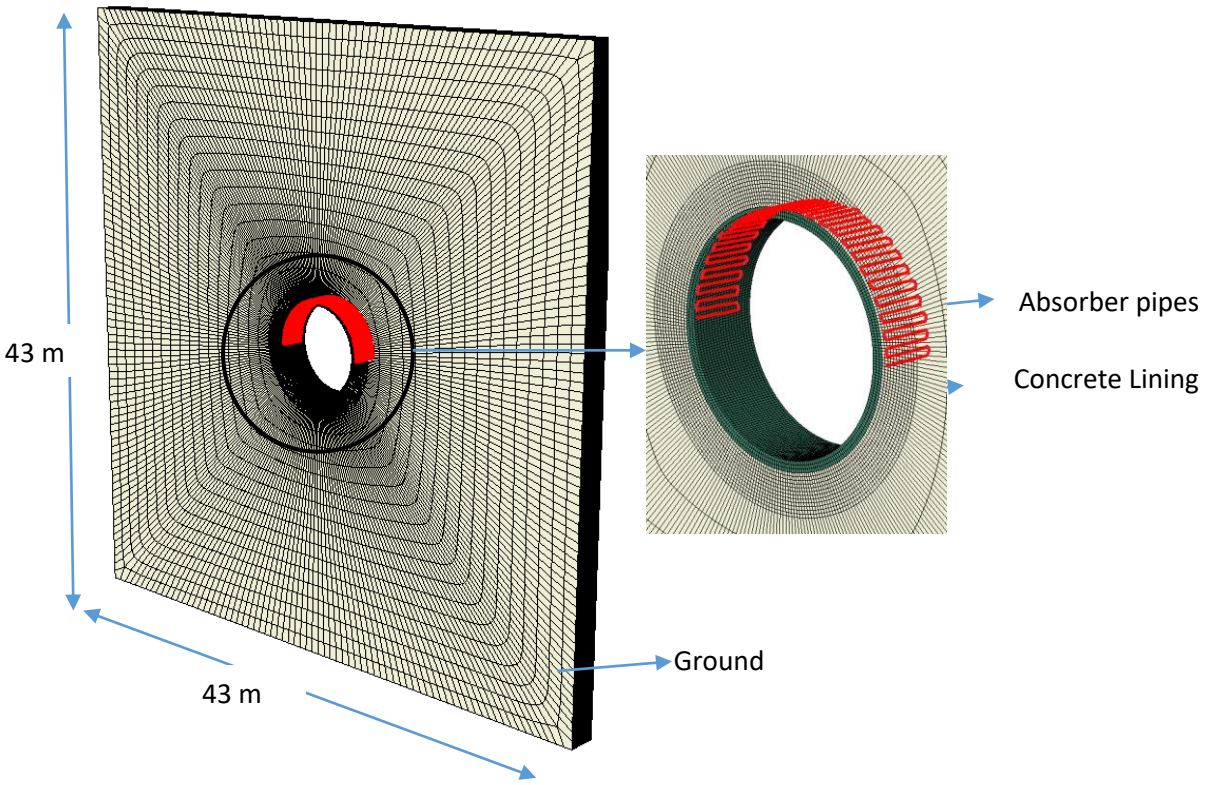

Fig. 9. Geometry and dimensions of the 3D model (parametric analysis)

Table 3. Mesh independence study.

Number of elements	Steady state outlet temperature (℃)
155001	5.724
163244	5.831
178111	5.872
184400	5.931
195444	5.932
200122	5.932

4. Results and Discussion

The daily IRs considered were 16/8, 12/12 and 8/16. The model calculates the outlet temperature of fluid at a given time, hence the extractable heat Q can be computed using the following equation [38]:

$$Q = \dot{m} c_w |T_{wO} - T_{wi}| \quad (10)$$

where $\dot{m}$ is the mass flow rate, T_{wi} is the inlet temperature of the pipe and T_{wO} is the outlet temperature. The average extractable heat is calculated by computing the average thermal output in a given period divided by the tunnel surface area, as

$$Q_{total} = \int_0^t Q(t)dt\ /A \tag{11}$$

where t = number of days under study and A is the tunnel surface area.

The number of days simulated in this study was considered sufficient to study the effect of intermittent operation and tunnel airflow whilst reducing computational time.

4.1. Outlet Fluid Temperature History

Fig. 10 shows the simulated change in outlet fluid temperature with time plotted for the first and last 10 days and between day 40 and 50 (when air temperature is minimum) during the heat extraction period. For the continuous operation, the outlet temperature reduces with time in the early period before reaching a quasi-steady state. The outlet temperature at the end of day 1 in continuous mode is 6.5℃ when the tunnel air temperature is at 15.3℃. The outlet temperature attains a value of 5.6℃ on day 45 when air temperature inside the tunnel is minimum (13.5℃), it shows that while running in continuous mode, for a 1.8℃ decrease in tunnel air temperature, the outlet temperature reduces by 0.9℃.

For a given day during daily intermittent operation, the outlet temperature decreases with time but tends towards a steady state before falling to 4℃ (initial inlet temperature) corresponding to the off period. Since the intermittent operation does not run long enough for the outlet temperature of the working fluid to reach a steady state, the difference in the outlet temperature can be explained from the outlet temperature-time gradient. The gradient increases with increasing IR and also changes with time for a given IR due to the effect of prolonged heating and the varying tunnel air temperature.

The average outlet temperature differs for different ratios, on day one while running the 8 on 16 off operation an average outlet temperature of 10.6℃ was obtained and in 16 on 8 off operation, an average temperature of 9.9℃ was obtained, resulting in a 0.7℃ difference. The difference between the average temperature increases as the number of days of operation increases and a difference of 0.9℃ was obtained at the end of the 90 days. The knowledge of the outlet temperature for different intermittent modes can serve as a control strategy for working out the ideal heat pump working condition by optimising the condensing and the evaporating temperature.

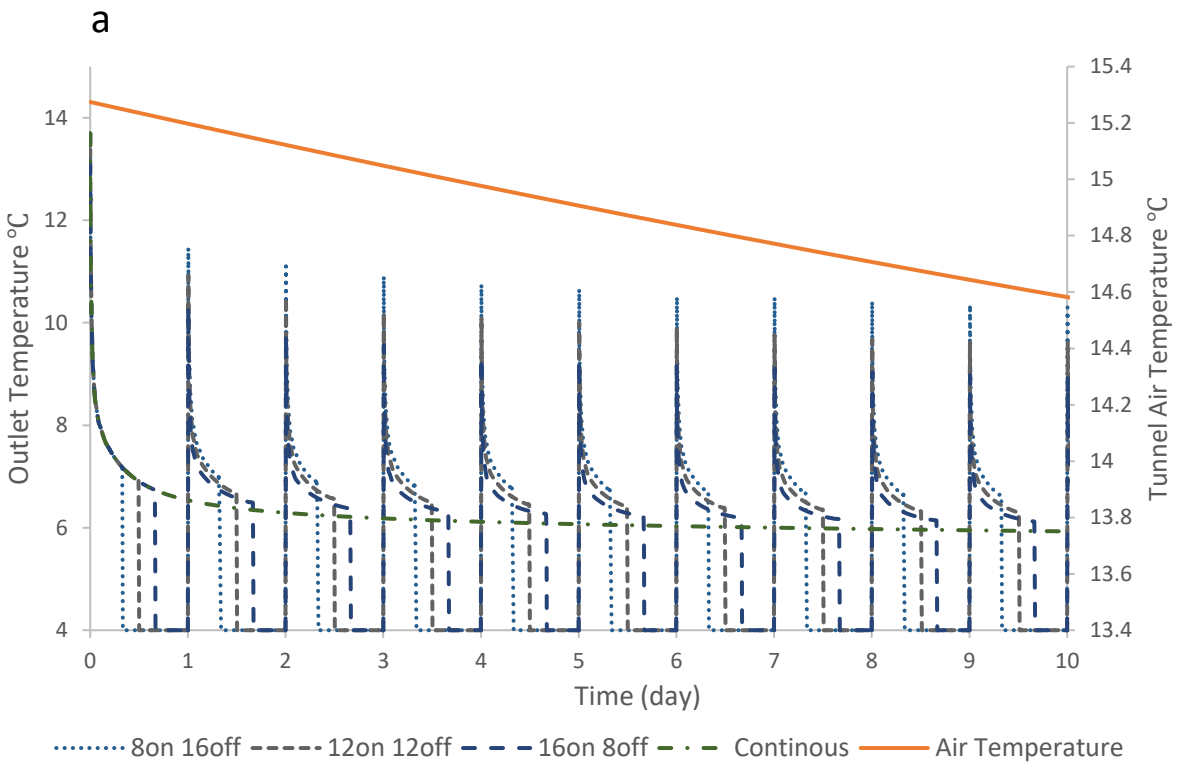
a
Outlet Temperature °C
Tunnel Air Temperature °C
Time (day)
8on 16off
12on 12off
16on 8off
Continous
Air Temperature

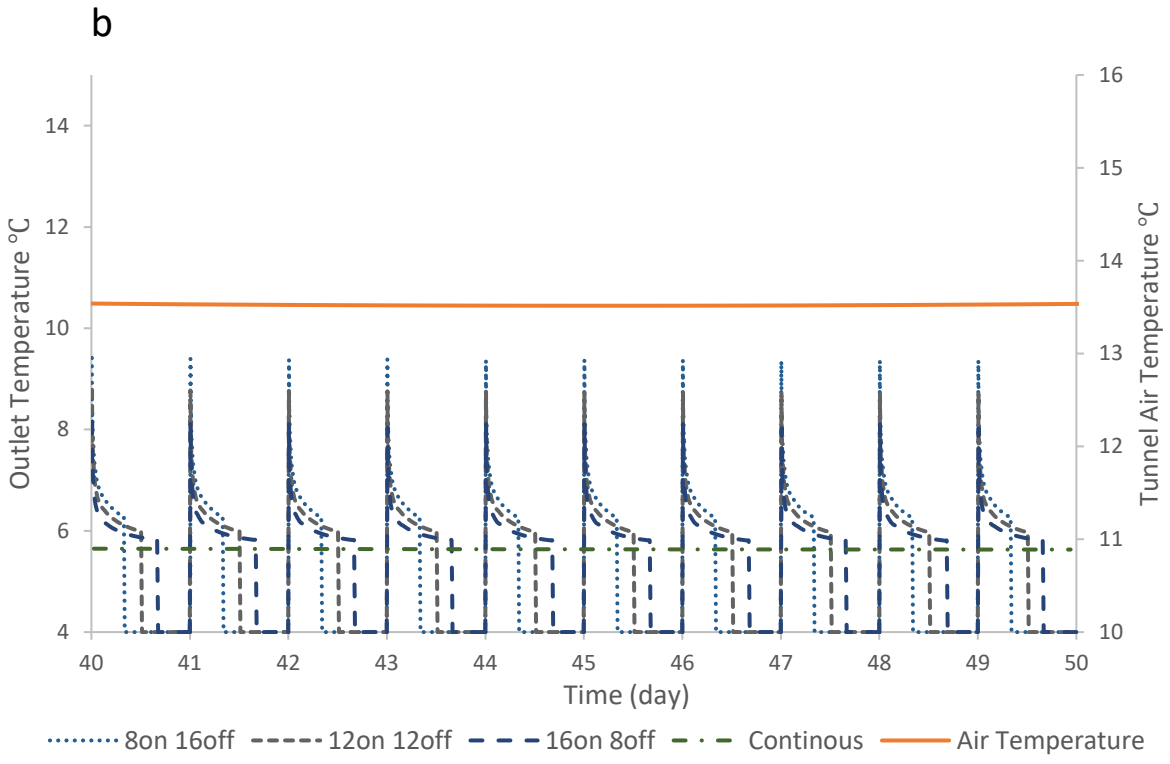
b
Outlet Temperature °C
Tunnel Air Temperature °C
Time (day)
8on 16off
12on 12off
16on 8off
Continous
Air Temperature

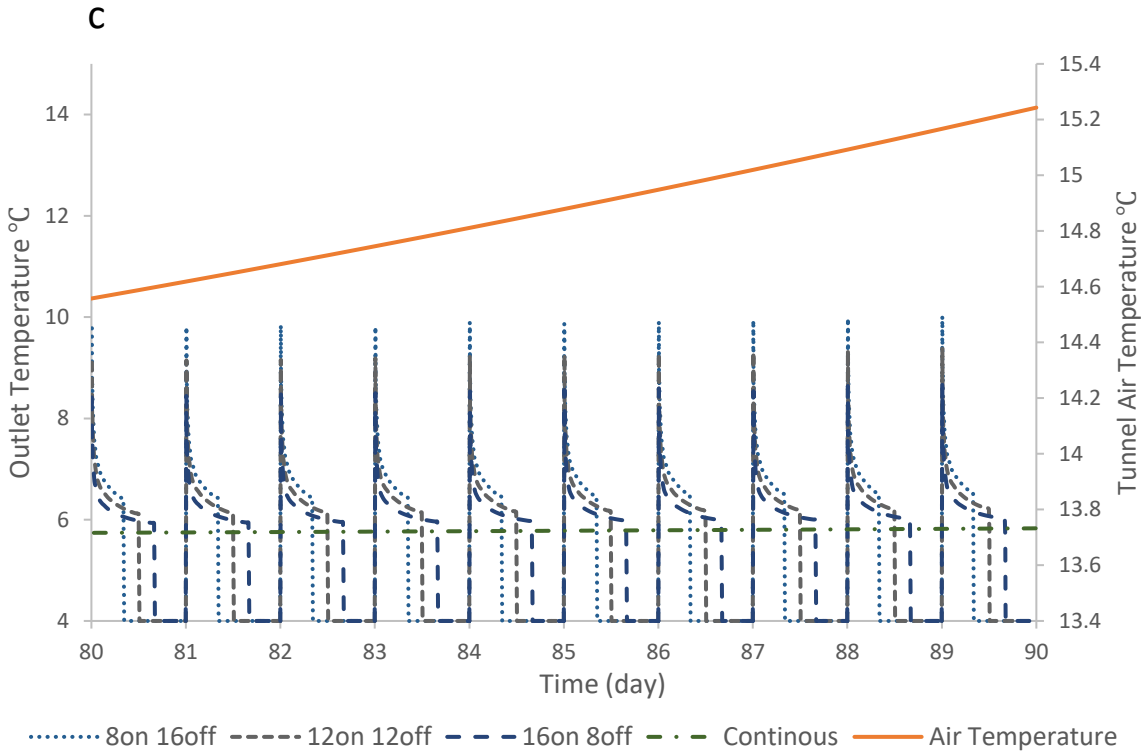

Fig. 10. Outlet fluid temperature history and Air Temperature (a) first 10days (b) day 40 to 50 (c) last 10days

4.2. Intermittent heating versus continuous heating

From the temperature results, the heat extraction rate was computed using **Eqn. (11)**. The chart of average heat exchange rate versus running time for intermittent operation and continuous operation is shown in **Fig. 11.** The average heat extracted increases with increasing IR, the difference between daily extracted heat for different IRs changes with time, due to different recovery times. During the initial stages, e.g. after 5 days of extraction, there was a 14.2% difference in the average thermal output between IR= 1 (12 on 12 off) and IR=2 (8 on, 16 off) and approximately the same percentage difference between IR=1 and IR=0.5 (16 on 8 off). At the end of the 90 days, the average heat extracted per square meter has more than doubled for IR=2 compared to continuous operation. Expectedly, the maximum average heat extracted for all the operation considered occurred on day 1 when the air temperature was at it maximum (**Fig. 9**).

In addition, **Fig. 11** also shows that for all operation modes, the heat extracted dropped significantly after day one. The heat flux from the tunnel air was not enough to thermally recharge the surrounding soil (i.e. it could not avoid the observed extracted heat drop) in the case examined. However, it should be noted that a different or varying heat transfer coefficient between the tunnel lining and air would result in a different transient thermal response.

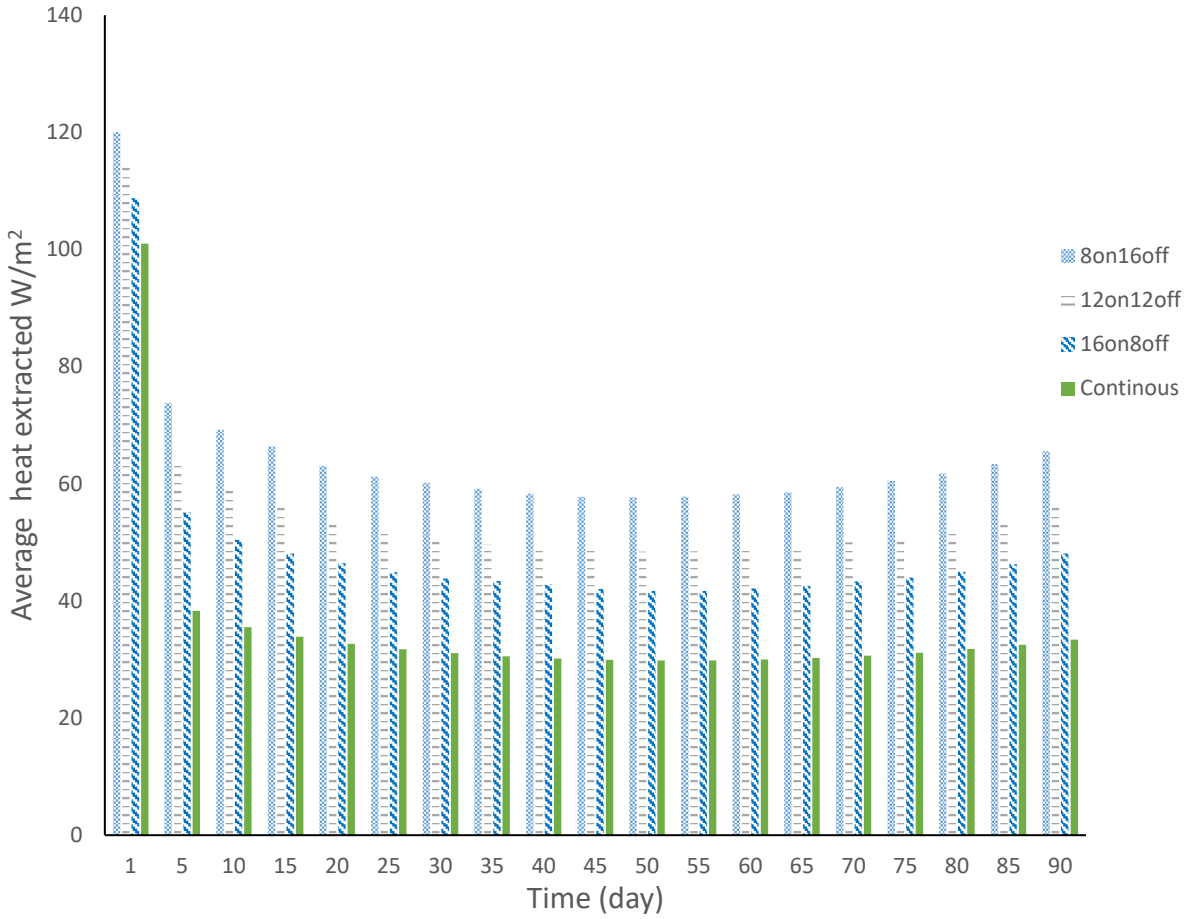

Fig. 11. Daily Average heat extracted plotted for 90 days of simulation

4.3. Influence of Tunnel air Temperature

Fig. 12 illustrates how the periodic change in the tunnel air temperature affects the thermal output of the tunnel. For all operations modes, the average heat extracted decreases with decreasing air temperature and increases as the air temperature increase. The overall trend shows that for the period of air temperature cycle considered, the average thermal output for the operation has identical oscillation as the tunnel air temperature. The average heat extracted on day one when the air temperature is maximum (15.3℃) are 120 W/m^2, 114 W/m^2, 108 W/m^2, 101 W/m^2 for IR 2, 1, 0.5 and continuous operation respectively. For IR 2, it can be seen that the average daily heat extracted has dropped to 57.8 W/m^2 when the air temperature dropped from 13.5℃. Also for IR 1 the heat output dropped to 48.7 W/m^2, similar trend can be said for IR 0.5, with the heat output dropping to 42W/m^2 from 108 W/m^2.

The above observed trends show that in hot tunnels, the heat extracted rate depends on the tunnel air temperature. The influence of tunnel air flow and temperature and profile should be included when estimating the geothermal potential of energy tunnels.

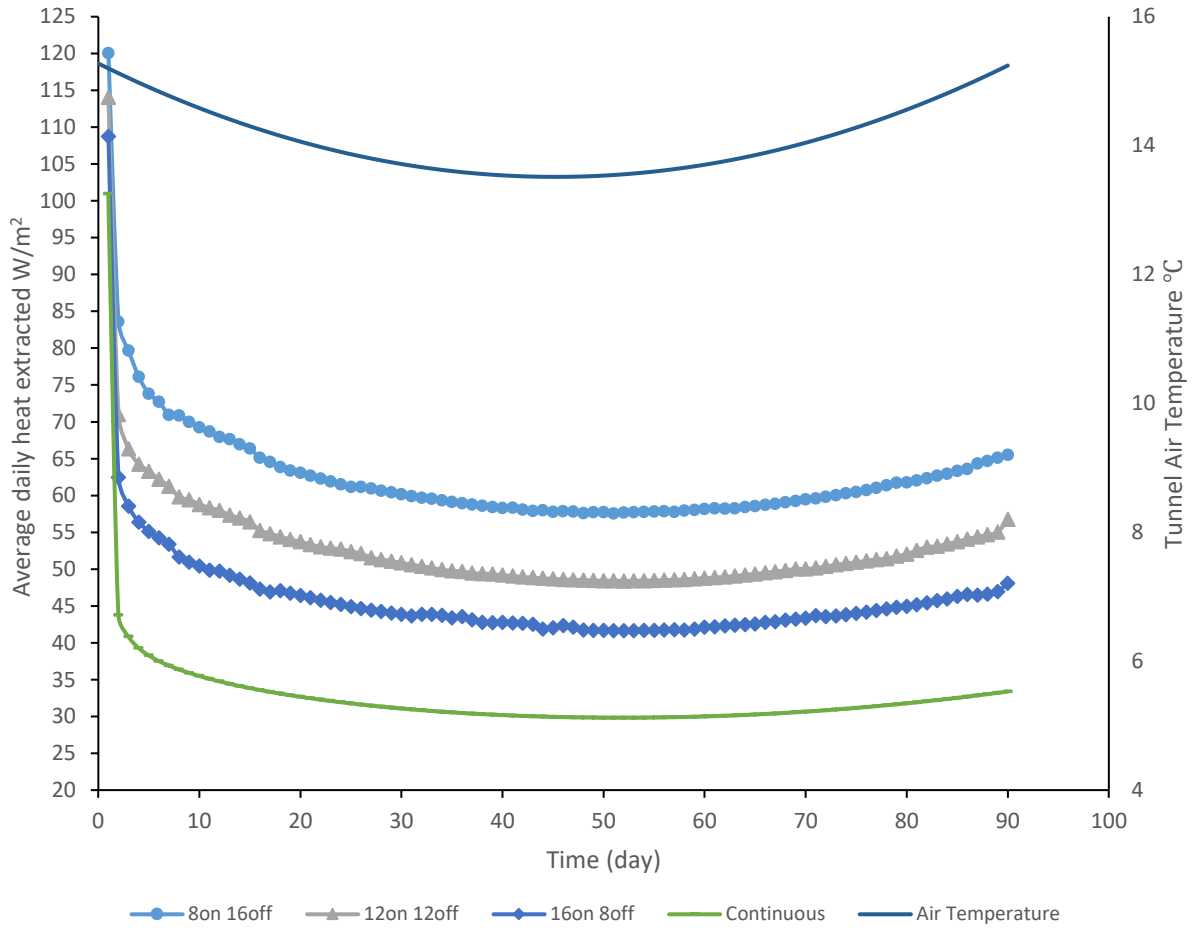

Fig. 12. Effect of air temperature on average heat extracted plotted for 90 days of simulation

4.4. Ground temperature

As regards ground temperature, energy tunnel continuous operation brings about a more extended perturbation in the surrounding soil compared to intermittent operation modes. To illustrate this effect, temperature contours for continuous operation are shown in **Fig. 13** after 90 days of heat extraction in a tunnel transversal cross-section. The figure shows the difference between the temperature field in the upper section and the lower section of the tunnel. This temperature distribution is due to 3/4th of the tunnel lining being thermally activated. The bottom part (1/4th) of the tunnel would be used by rail or road track and cabling and therefore absorber pipes cannot be placed in the bottom part under the track where they would be subjected to significant dynamic loading, that may result in damage and leakage of the pipes. Higher temperatures than the undistrurbed value are attained at the bottom of the tunnel, mainly due to the tunnel air boundary condition.

The combined effect of the intermittent operation and varying air temperature on the surrounding soil temperature can be inferred from **Fig. 14**, where the concrete and soil spatial temperature profile is plotted at 30 days intervals along the reference line shown in **Fig. 13** (this line corresponds to the line of maximum temperature change along the tunnel cross-section). **Fig. 14** shows that for all operation modes, after day one (**Fig. 14a**), the temperature perturbation reaches a short distance

(0.5 m) from the tunnel interior, but this distance increases with time. At the end of day 30, the area affected by the heat exchange process is approximately 5.5 m from the tunnel interior. On day 60, the distance extends to 7 m, and after 90 days the temperature change extends to 8.4 m.

As expected for lower IRs, the magnitude of the ground temperature change are higher at the end of the extraction period with higher amplitudes at the end of the off periods. The graphs show the extent of soil temperature recovery during the off periods; however, since there is a variation of tunnel air temperature, the heat gained at the tunnel wall diffuses into the lining, thus helping the recovery process. Hence, the rate of temperature drop and recovery in the soil is also influenced by tunnel air temperature changes, in addition to the heat exchange with absorber pipes.

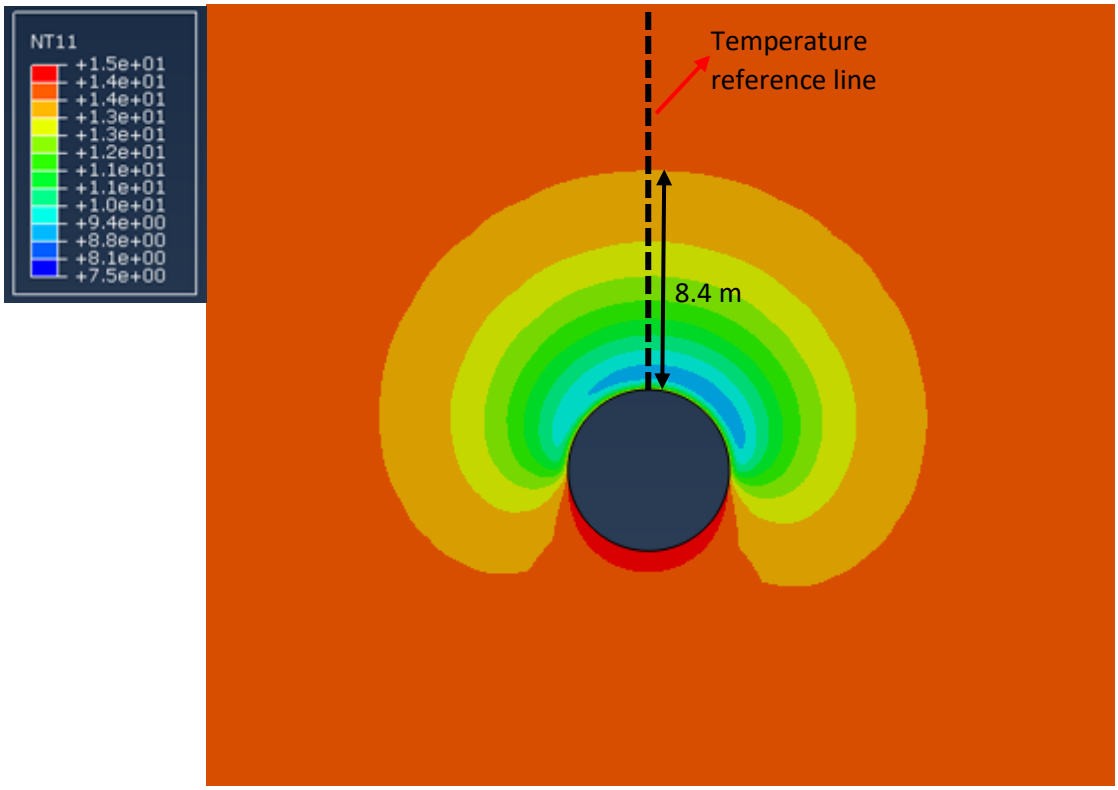

Fig. 13. 2-D view of the model result after 90 days of continuous heat extraction.

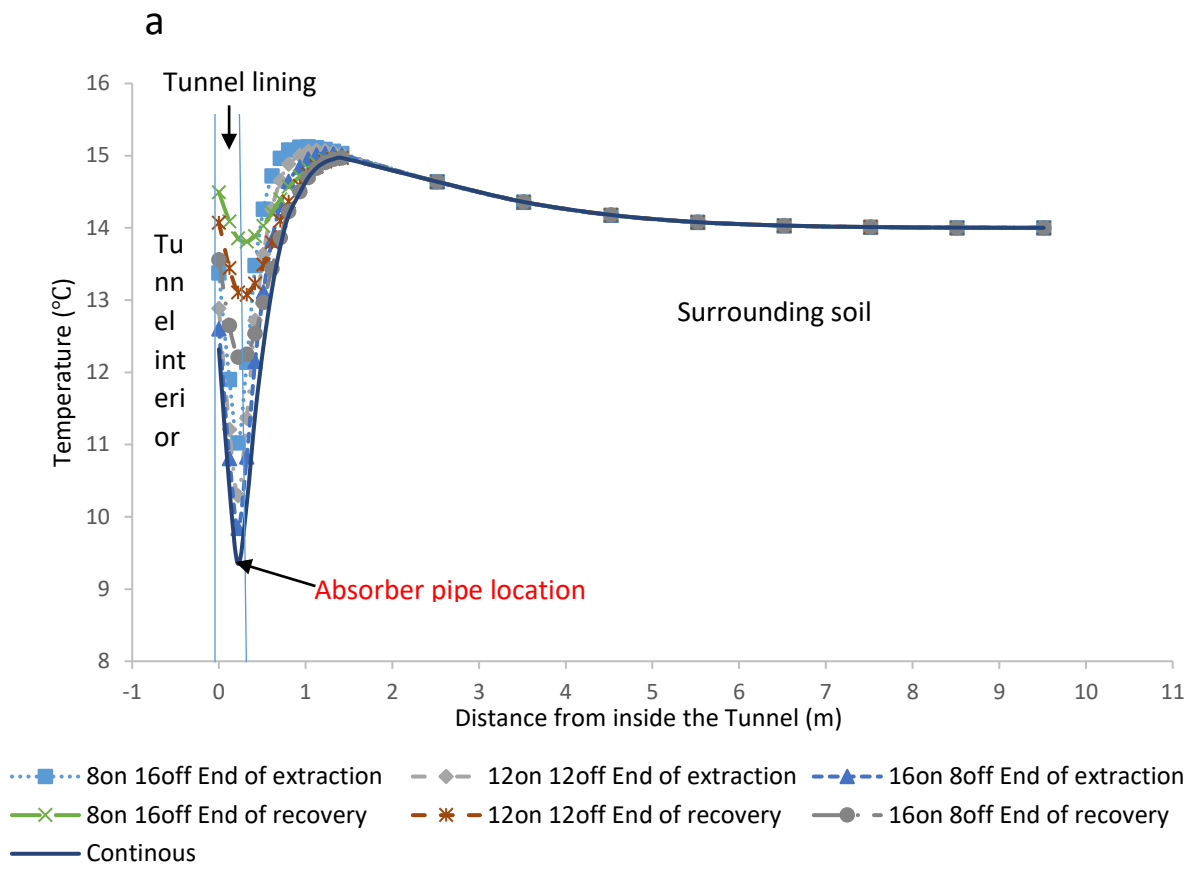
a
Tunnel lining
Tu
nn
el
int
eri
or
Surrounding soil
Absorber pipe location
Temperature (°C)
Distance from inside the Tunnel (m)
8on 16off End of extraction
12on 12off End of extraction
16on 8off End of extraction
8on 16off End of recovery
12on 12off End of recovery
16on 8off End of recovery
Continous

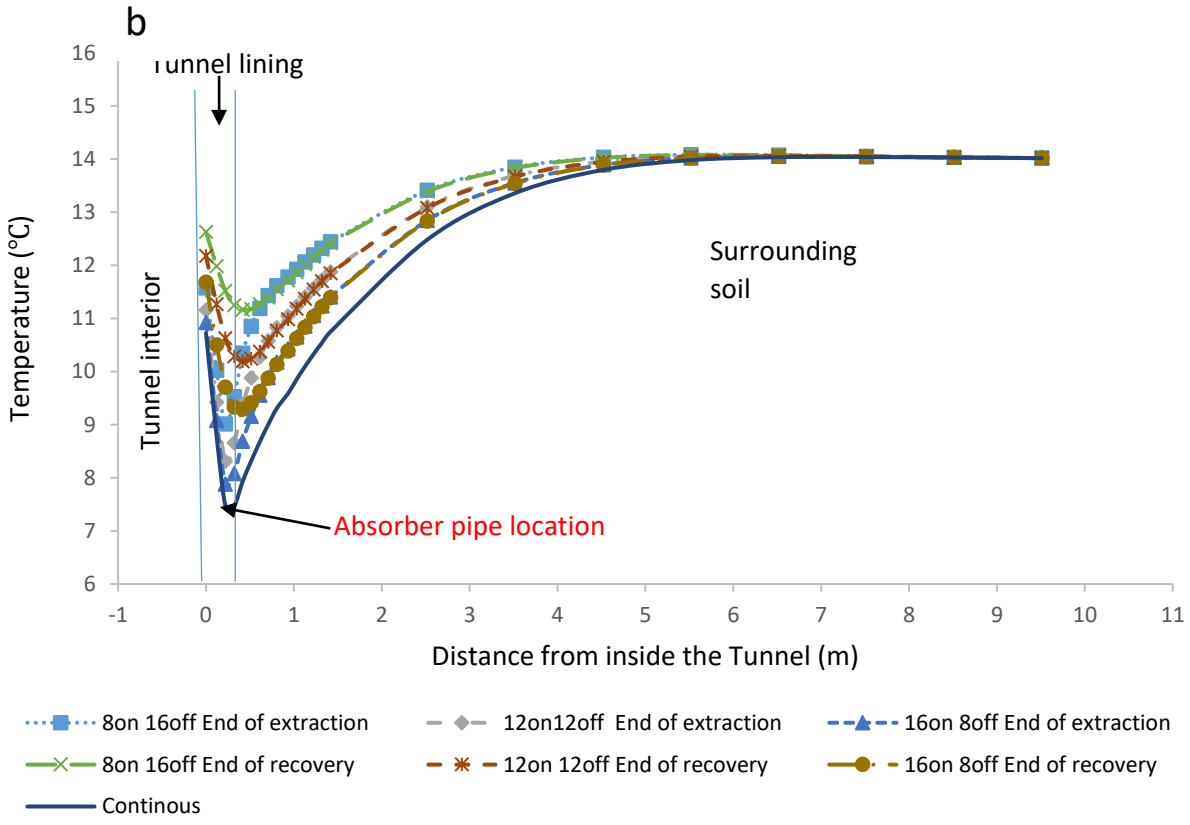
b
Tunnel lining
Tunnel interior
Surrounding
soil
Absorber pipe location
Temperature (°C)
Distance from inside the Tunnel (m)
8on 16off End of extraction
12on12off End of extraction
16on 8off End of extraction
8on 16off End of recovery
12on 12off End of recovery
16on 8off End of recovery
Continous

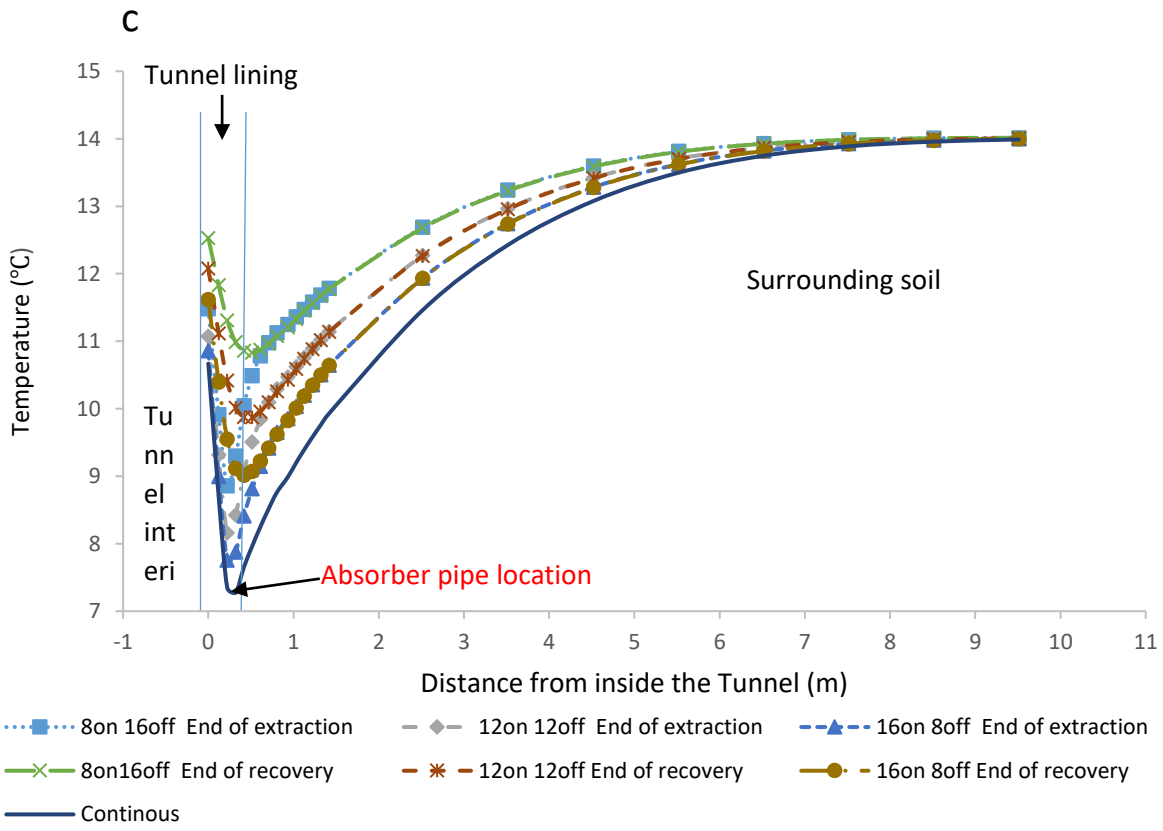

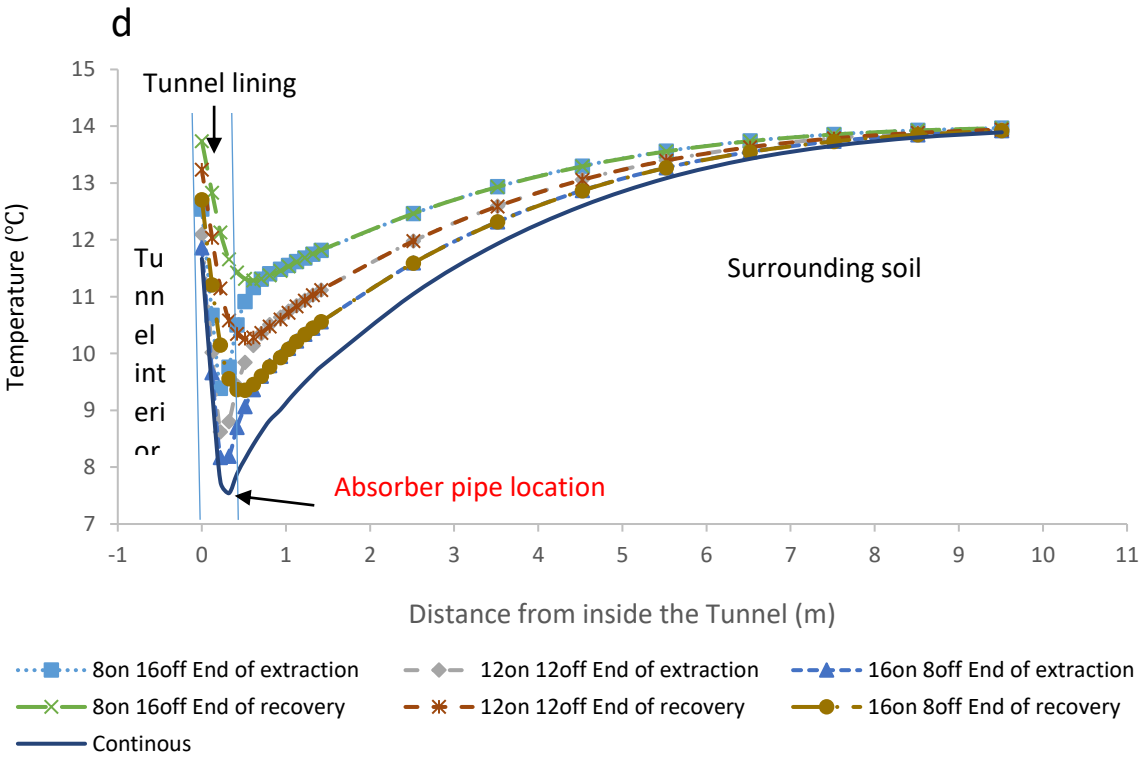

Fig. 14. Ground temperature distribution

(a) After 1 day of extraction (b) After 30 days of extraction (c) After 60 days of extraction (d) After 90 days of extraction.

From the results presented above it can be deduced that after a prolonged period of heat extraction (i.e. 90 days), and considering the changes in tunnel air temperature, adopting the highest IR causes soil to recover the initial thermal equilibrium more quickly, hence reducing the overall impact of the heat extraction process.

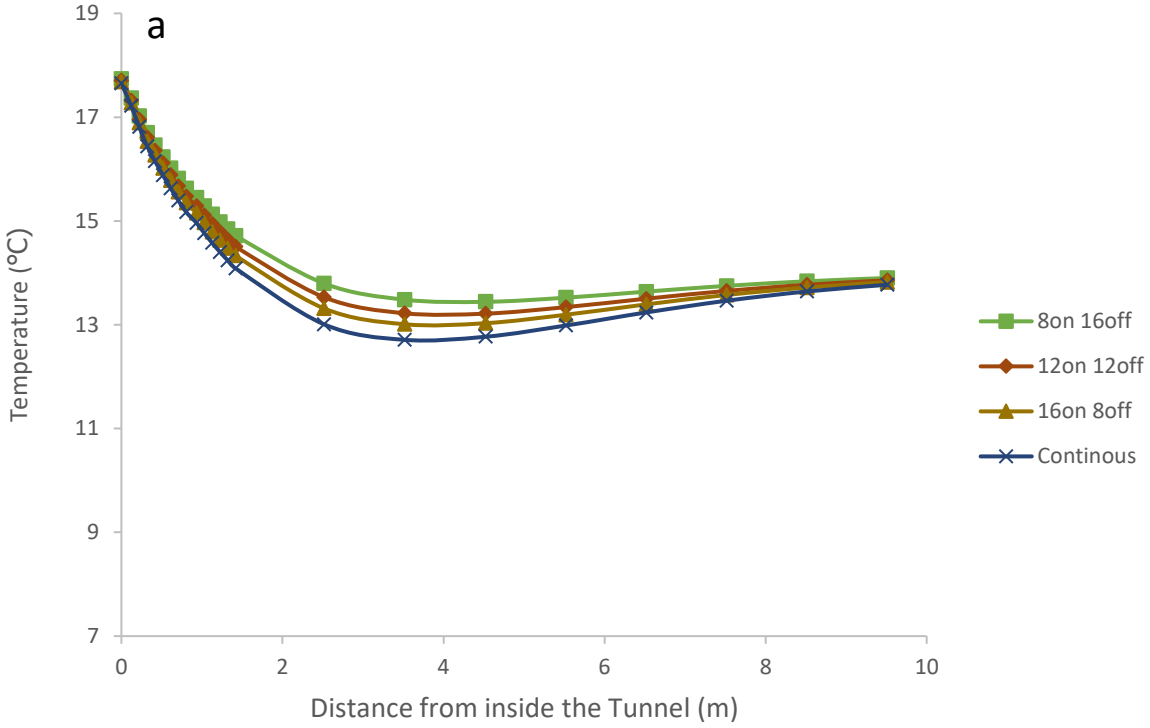

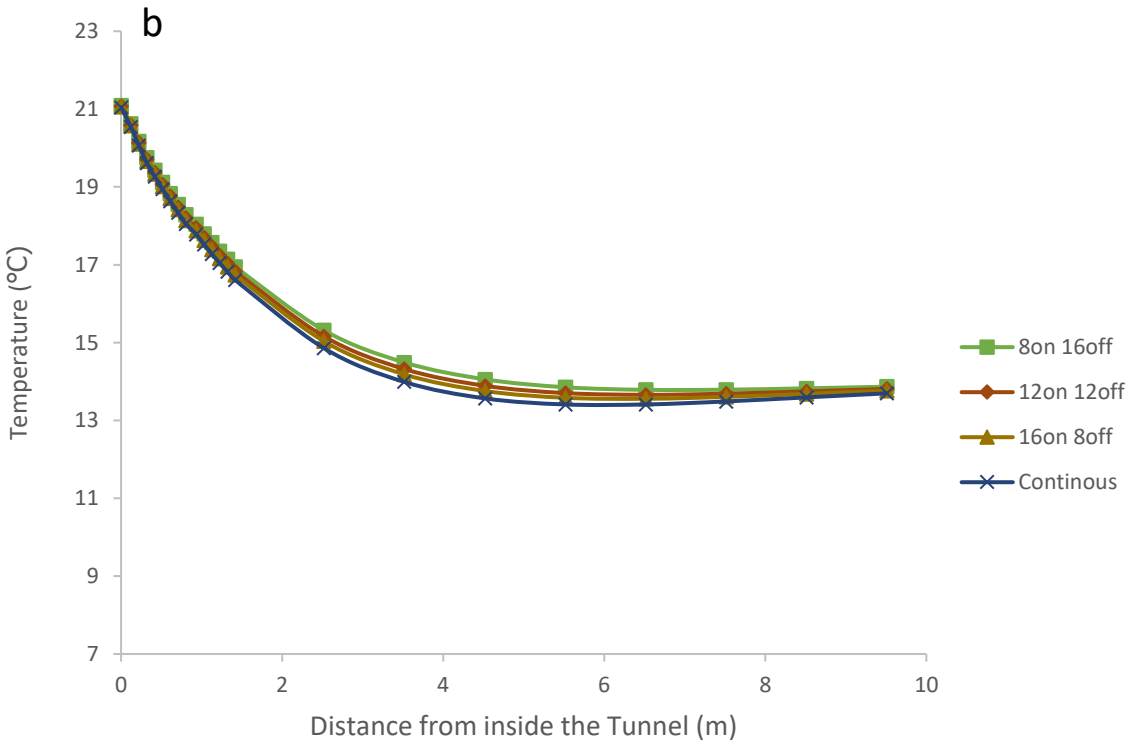

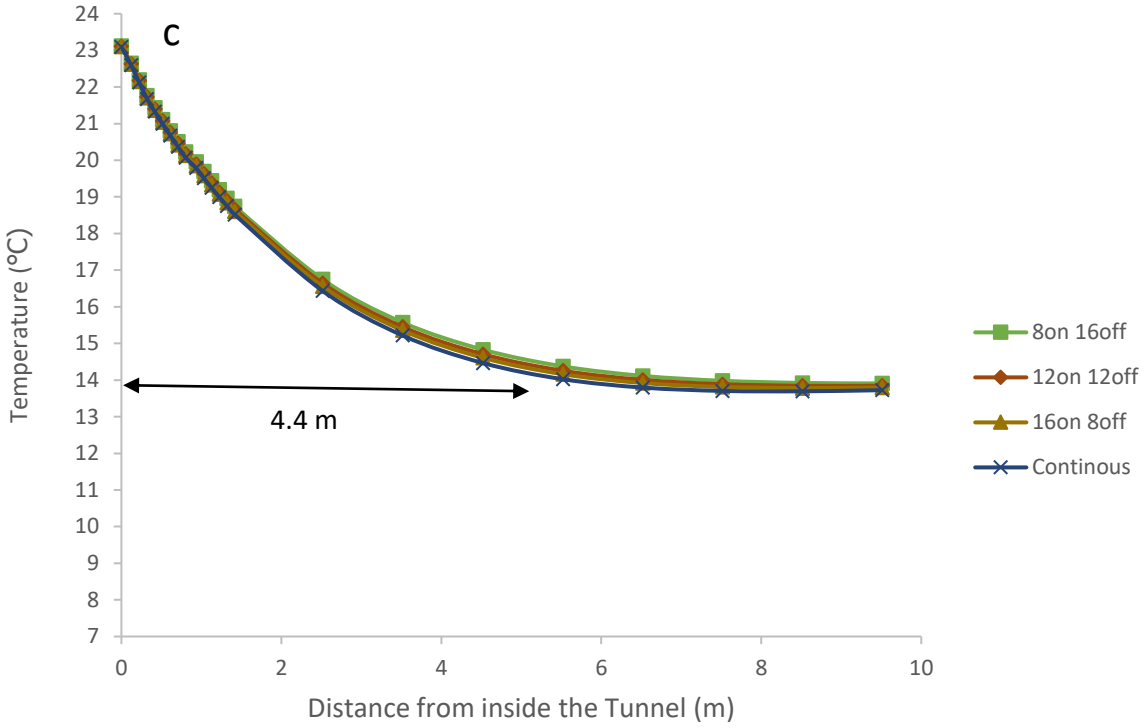

Fig. 15. Ground temperature distribution after 90 days period without heat extraction.

(a) After 30 days of recovery (b) After 60 days of recovery (c) After 90 days of recovery

Furthermore, the combined effect of heat extraction and of tunnel air temperature change on the surrounding soil was evaluated by simulating recovery periods without heat extraction. As explained above, the rate of heat extraction and soil recovery depends on the IR adopted and on temperature variations inside the tunnel. The progress of the thermal recovery process in the surrounding soil (after heat extraction) is noticeable after 30 days with a progressive improvement after 60days (**Fig. 15**). The rate of recovery is also related to the IR, with higher ratios recovering faster as expected due to lower thermal disturbance. After 90 days without heat extraction for all the simulated operation modes, the surrounding soil can be considered to have thermally recovered. On the other hand, it can be observed that the heat flux from the tunnel air alone has a comparable impact on the surrounding soil relative to the heat extraction process. In fact, while the maximum temperature change (from undisturbed soil temperature) during continuous operation after 90 days was 6.5°C and the temperature perturbation extended up to a distance of 8.4 m from the concrete lining (**Fig. 13** and **Fig. 14**), the effect of hot tunnel air could be measured at a distance of 4.4 m (**Fig. 15**) from the concrete lining, with a maximum change of 9°C relative to the initial soil temperature.

5. Conclusion

The operation of an energy tunnel for heat extraction in intermittent modes under varying tunnel air temperature was investigated in this work. An improved 3-D Finite Element transient model with bespoke subroutines was developed to simulate the heat transfer in the tunnel, and was validated against experimental data.

The following observations can be drawn from this study:

- Running the system intermittently increases the thermal output, and higher IRs bring about higher average daily thermal outputs. Intermittent operations are characterised by a lower ground temperature drop and a higher recovery rate compared to a continuous operation, resulting in a more efficient system.
- The required running time for the heat pump will be different for different applications. However, for a continuous heating demand, an optimum IR should be determined and an auxiliary source may be used to meet the energy demand during the off period. The selected ratio should improve performance and reduce cost by minimising the soil temperature disturbance and reduce the overall energy consumption.
- The temperature time history of the air inside the tunnel also affects the heat exchange process, and it is important to include this when estimating the geothermal potential of an energy tunnel. For tunnels without existing data on air temperature, forecasting the temperature profile (depending on tunnel use and environmental condition) is essential when planning the GHE system design.
- Predictions about the soil temperature evolution during a 90 days period without heat extraction show that the ground has thermally recovered from previous disturbance. Results also show that the heat flux from the hot tunnel interior alone may have a comparable impact on the surrounding soil temperature disturbance compared to the heat extraction operation. This is an important finding as it serves as a basis for working out optimum seasonal intermittent operation strategies in energy tunnels.
- Further studies should be conducted to develop models capable of determining the optimal operation strategies. These models should be based on site conditions, economic considerations and consumer demands. From the numerical modelling point of view, further developments should include groundwater convection, to be able to apply this type of thermal efficiency analyses to energy tunnels located within flowing aquifers.

Acknowledgment

Funding: This work was supported by the Department of Civil and Environmental Engineering, Faculty of Engineering and Physical Sciences, University of Surrey, Guildford.

Declaration of interest: None.

References

[1] Buhmann, P., Moormann, C., Westrich, B., Pralle, N., and Friedemann, W., 2016, "Tunnel geothermics-A German experience with renewable energy concepts in tunnel projects," Geomech. Energy Environ., 8, pp. 1-7.
[2] Brandl, H., 2006, "Energy foundations and other thermo-active ground structures," Geotechnique, 56(2), pp. 81-122.
[3] Brandl, H., 2016, "Geothermal Geotechnics for Urban Undergrounds," 15th International Scientific Conference Underground Urbanisation as a Prerequisite for Sustainable Development, 165, pp. 747-764.
[4] Barla, M., Di Donna, A., and Insana, A., 2019, "A novel real-scale experimental prototype of energy tunnel," Tunn. Undergr. Space Technol., 87, pp. 1-14.
[5] Colino, M. R., Rosenstein, E. B., and Asme, 2017, "A NEW ADVANCE IN TUNNEL VENTILATION DESIGN PLANNING," Proceedings of the Asme Joint Rail Conference, 2017, p. 10.
[6] Yang, C., Peng, F. L., Xu, K., and Zheng, L. N., 2019, "Feasibility study on the geothermal utility tunnel system," Sust. Cities Soc., 46, p. 8.
[7] Di Donna, A., Cecinato, F., Loveridge, F., and Barla, M., 2017, "Energy performance of diaphragm walls used as heat exchangers," Proc. Inst. Civil Eng.-Geotech. Eng., 170(3), pp. 232-245.
[8] Davies, G., Boot-Handford, N., Curry, D., Dennis, W., Ajileye, A., Revesz, A., and Maidment, G., 2019, "Combining cooling of underground railways with heat recovery and reuse," Sust. Cities Soc., 45, pp. 543-552.
[9] Ampofo, F., Maidment, G., and Missenden, J., 2004, "Underground railway environment in the UK Part 2: Investigation of heat load," Appl. Therm. Eng., 24(5-6), pp. 633-645.
[10] Barrow, H., and Pope, C. W., 1987, "A SIMPLE ANALYSIS OF FLOW AND HEAT-TRANSFER IN RAILWAY TUNNELS," Int. J. Heat Fluid Flow, 8(2), pp. 119-123.
[11] Zhang, X. F., Yu, W. B., Wang, C., and Liu, Z. Q., 2006, "Three-dimensional nonlinear analysis of coupled problem of heat transfer in the surrounding rock and heat convection between the air and the surrounding rock in the Fenghuo mountain tunnel," Cold Reg. Sci. Tech., 44(1), pp. 38-51.
[12] Sadokierski, S., and Thiffeault, J., 2007, "Title."
[13] Barla, M., Di Donna, A., and Perino, A., 2016, "Application of energy tunnels to an urban environment," Geothermics, 61, pp. 104-113.
[14] Faizal, M., Bouazza, A., and Singh, R. M., 2016, "An experimental investigation of the influence of intermittent and continuous operating modes on the thermal behaviour of a full scale geothermal energy pile," Geomech. Energy Environ., 8, pp. 8-29.
[15] Lu, F. B., Fu, Y. Z., and Shi, L., 2015, "Analysis of the Ground Adjustment Ability of Ground Source Heat Pump Systems during Intermittent Operation in Summer," Proceedings of the 2015 International Forum on Energy, Environment Science and Materials, 40, pp. 6-9.
[16] Zhang, L. F., Zhang, Q., Li, M., and Du, Y. X., 2015, "A new analytical model for the underground temperature profile under the intermittent operation for Ground-Coupled Heat Pump systems," Clean, Efficient and Affordable Energy for a Sustainable Future, 75, pp. 840-846.
[17] Agbossou, A., Souyri, B., and Stutz, B., 2018, "Modelling of helical coil heat exchangers for heat pump applications: Analysis of operating modes and distance between heat exchangers," Appl. Therm. Eng., 129, pp. 1068-1078.
[18] Liu, L., Yu, Z., Zhang, H., and Yang, H. W., 2016, "Performance improvements of a ground sink direct cooling system under intermittent operations," Energy Build., 116, pp. 403-410.
[19] Zhang, L. L., Zhao, L., Yang, L., and Hu, S. T., 2015, "Analyses on soil temperature responses to intermittent heat rejection from BHEs in soils with groundwater advection," Energy Build., 107, pp. 355-365.
[20] Li, C. F., Mao, J. F., Xing, Z. L., Zhou, J., and Li, Y., 2016, "Analysis of Geo-Temperature Restoration Performance under Intermittent Operation of Borehole Heat Exchanger Fields," Sustainability, 8(1), p. 14.

[21] Yang, W. B., Liang, X. F., Shi, M. H., and Chen, Z. Q., 2014, "A NUMERICAL MODEL FOR THE SIMULATION OF A VERTICAL U-BEND GROUND HEAT EXCHANGER USED IN A GROUND-COUPLED HEAT PUMP," Int. J. Green Energy, 11(7), pp. 761-785.
[22] Zarrella, A., Emmi, G., and De Carli, M., 2015, "Analysis of operating modes of a ground source heat pump with short helical heat exchangers," Energy Conv. Manag., 97, pp. 351-361.
[23] Chen, J., Xu, L. H., Hu, P. F., Zhu, N., and Ieee, 2013, "Comparative Study of Intermittent Operating Conditions for Hybrid Ground-Source Heat Pump," 2013 International Conference on Materials for Renewable Energy and Environment (Icmree), Vols 1-3, pp. 942-946.
[24] He, L., and Sun, H. J., 2009, "Energy-saving potential analysis for teaching building with intermittent heating system in university of Tianjin," J. Cent. South Univ. Technol., 16, pp. 111-117.
[25] Chen, F., Mao, J. F., Chen, S. Y., Li, C. F., Hou, P. M., and Liao, L., 2018, "Efficiency analysis of utilizing phase change materials as grout for a vertical U-tube heat exchanger coupled ground source heat pump system," Appl. Therm. Eng., 130, pp. 698-709.
[26] Gao, Q., Li, M., and Yu, M., 2010, "Experiment and simulation of temperature characteristics of intermittently-controlled ground heat exchanges," Renew. Energy, 35(6), pp. 1169-1174.
[27] Kim, D., Kim, G., and Baek, H., 2017, "Experimental and numerical investigation of thermal properties of cement-based grouts used for vertical ground heat exchanger," Renew. Energy, 112, pp. 260-267.
[28] Zhang, C. B., Yang, W. B., Yang, J. J., Wu, S. C., and Chen, Y. P., 2017, "Experimental Investigations and Numerical Simulation of Thermal Performance of a Horizontal Slinky-Coil Ground Heat Exchanger," Sustainability, 9(8), p. 22.
[29] Xia, C. C., Sun, M., Zhang, G. Z., Xiao, S. G., and Zou, Y. C., 2012, "Experimental study on geothermal heat exchangers buried in diaphragm walls," Energy Build., 52, pp. 50-55.
[30] Pei, G. H., and Zhang, L. Y., 2016, "Heat transfer analysis of underground U-type heat exchanger of ground source heat pump system," SpringerPlus, 5, p. 15.
[31] Choi, J. C., Lee, S. R., and Lee, D. S., 2011, "Numerical simulation of vertical ground heat exchangers: Intermittent operation in unsaturated soil conditions," Comput. Geotech., 38(8), pp. 949-958.
[32] Chong, C. S. A., Gan, G., Verhoef, A., Garcia, R. G., and Vidale, P. L., 2013, "Simulation of thermal performance of horizontal slinky-loop heat exchangers for ground source heat pumps," Appl. Energy, 104, pp. 603-610.
[33] Yuan, Y. P., Cao, X. L., Wang, J. Q., and Sun, L. L., 2016, "Thermal interaction of multiple ground heat exchangers under different intermittent ratio and separation distance," Appl. Therm. Eng., 108, pp. 277-286.
[34] Hu, Y. N., Kong, N., and Hu, S. S., 2013, "Hourly Simulation Study of Intermittent Operating Conditions for Ground Heat Exchanger in the Hot Summer and Warm Winter Areas," Advances in Environmental Technologies, Pts 1-6, 726-731, pp. 3580-3587.
[35] Li, C. F., Mao, J. F., Zhang, H., Xing, Z. L., Li, Y., and Zhou, J., 2017, "Numerical simulation of horizontal spiral-coil ground source heat pump system: Sensitivity analysis and operation characteristics," Appl. Therm. Eng., 110, pp. 424-435.
[36] Cao, X. L., Yuan, Y. P., Sun, L. L., Lei, B., Yu, N. Y., and Yang, X. J., 2015, "Restoration performance of vertical ground heat exchanger with various intermittent ratios," Geothermics, 54, pp. 115-121.
[37] Cecinato, F., and Loveridge, F. A., 2015, "Influences on the thermal efficiency of energy piles," Energy, 82, pp. 1021-1033.
[38] Bergman, T. L., and Incropera, F. P., 2011, Fundamentals of heat and mass transfer, Wiley, Hoboken, NJ.
[39] Loveridge, F., and Cecinato, F., 2016, "Thermal performance of thermoactive continuous flight auger piles," Environ Geotech-J, 3(4), pp. 265-279.
[40] Zhang, G. Z., Xia, C. C., Sun, M., Zou, Y. C., and Xiao, S. G., 2013, "A new model and analytical solution for the heat conduction of tunnel lining ground heat exchangers," Cold Reg. Sci. Tech., 88, pp. 59-66.

[41] Clarke, B. G., Agab, A., and Nicholson, D., 2008, "Model specification to determine thermal conductivity of soils," Proc. Inst. Civil Eng.-Geotech. Eng., 161(3), pp. 161-168.
[42] Wang, L. H., Zou, X. C., Tao, H., Song, J., and Zheng, Y., 2017, "Experimental Study on Evolution Characteristics of the Heat Storage of Surrounding Soil in Subway Tunnels," 10th International Symposium on Heating, Ventilation and Air Conditioning, Ishvac2017, 205, pp. 2728-2735.
[43] Liu, X. C., Xiao, Y. M., Inthavong, K., and Tu, J. Y., 2014, "A fast and simple numerical model for a deeply buried underground tunnel in heating and cooling applications," Appl. Therm. Eng., 62(2), pp. 545-552.